JTTEE5 18:392–400
DOI: 10.1007/s11666-009-9303-8
1059-9630/$19.00 © ASM International

Effects of Temperature of In-flight Particles on Bonding and Microstructure in Warm-Sprayed Titanium Deposits

KeeHyun Kim, Makoto Watanabe, Jin Kawakita, and Seiji Kuroda

(Submitted October 27, 2008; in revised form January 22, 2009)

Micron-sized titanium particles were deposited on steel substrates by the warm spraying, which is a modified high velocity oxy-fuel (HVOF) spraying technique. In the process, nitrogen gas is mixed with the HVOF flame jet to lower the temperature of injected powder particles. Detailed observations of splats formed on polished substrates by using scanning electron microscopy (SEM) and transmission electron microscopy (TEM) were conducted to investigate the effects of particle temperature on the bonding of splats with the substrate and the microstructure within the splats. At lower nitrogen flow rates, the particles observed were heavily deformed and exhibited diverse splat morphologies and microstructures. At higher nitrogen flow rates, most of the particles were impacted in the solid state and the oxidation of particles was remarkably less. The TEM observation revealed distinctively different microstructures within the splats as well as the splat/substrate interfaces depending on whether the particle was molten or solid before the impact.

Keywords bonding, interfacial boundary, microstructure, splat morphology, titanium, warm spraying

1. Introduction

In conventional thermal spray processes, spraying materials are heated to high temperatures to induce complete or partial melting. However, it is often highly detrimental to materials such as titanium if operated in air because it is very reactive with gases such as oxygen and nitrogen at high temperature (Ref 1-3). The recently developed kinetic spraying process such as the cold spray can avoid melting the spraying materials. In the process, metallic powder particles accelerated in the supersonic stream of inert gas can be deposited on the substrate by the high velocity impact without melting the spraying powder (Ref 4). However, the critical velocity necessary to form the bonding of powder and substrate is relatively high for titanium due to its lower deformability related to its hcp crystal structure (Ref 5) and the reported microstructures of cold-sprayed titanium coating tend to be porous as compared to more easily sprayable materials such as copper and aluminum (Ref 4, 6). Therefore, the development of new method for making thick coatings or spraying near net-shaped components of titanium with high density is indispensable for many industrial applications (Ref 4).

KeeHyun Kim, Makoto Watanabe, Jin Kawakita, and **Seiji Kuroda**, Composites and Coatings Center, National Institute for Materials Science (NIMS), 1-2-1 Sengen, Tsukuba 305-0047, Japan. Contact e-mail: KIM.Keehyun@nims.go.jp.

By heating metallic materials to the range of temperature between 0.5 T_m and T_m, where T_m is the melting point of material, one can expect the significant increase of deformability and hence the increase of density of a coating layer without severe oxidation. It has been reported that the oxidation rate of thermal-sprayed particles during the flight increases dramatically once powder particles are melted due to the convective flow inside the particle, which exposes fresh molten metal continuously to the surface (Ref 7, 8). Recently, a novel kinetic spray process, called as the warm spray, based on this principle was developed (Ref 3, 9). As shown in Fig. 1, it is the modification of high velocity oxy-fuel (HVOF) spraying; the temperature of supersonic gas flow generated by the combustion of kerosene and oxygen is controlled by diluting the combustion flame with an inert gas such as nitrogen in the mixing chamber inserted between the combustion chamber and the powder feed ports. As a result, the sprayed particles can be heated to a moderate temperature below the melting point. Thus, the process can generate the flux of powder particles with the well-controlled temperature and velocity. However, the effects of temperature and velocity of the in-flight particles on the resultant microstructure have not been studied in detail.

The microstructure of sprayed particles affects various coating properties such as the mechanical and the electrical (Ref 10, 11). In addition, the observation of interfacial microstructure of the sprayed particles and the substrate is meaningful to understand the adhesion of sprayed particles onto a substrate. Although several studies have been conducted on the microstructure of thick cold-sprayed materials (Ref 12-17), few investigations of sprayed single particles as well as splat/substrate interface region have been reported because such research inevitably requires transmission electron microscopy

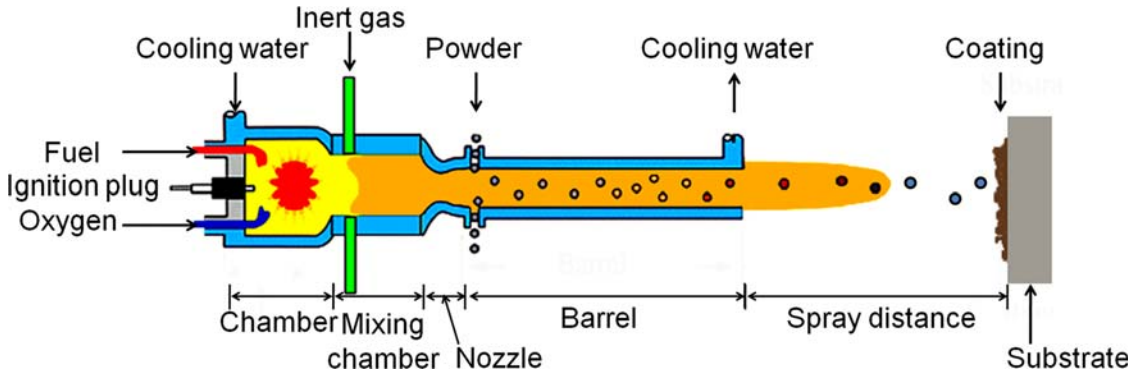

Fig. 1 Schematic diagram of warm spraying equipment

(TEM) and there used to be the difficulty in preparing a thin electron-transparent membrane out of such samples (Ref 18). Recently, however, the focused ion beam (FIB) lift-out technique using micro sampling functions has enabled the preparation of high quality cross-sectional TEM samples (Ref 19, 20). Especially, the delicate controlling of beam size and current in the FIB process can minimize the ion-induced damage generated by the normal ion-milling used to make a hole. Moreover, the process can make a large observable area, i.e., 5 μm (width) and 1-2 μm (height). Besides cutting, the FIB setup allows recording images, formed by electrons back-scattered by the incident Ga^+ ions, at any cutting stage. In this study, TEM samples were made by this technique. The detailed microstructure around the interface of titanium particle and steel substrate was observed in order to understand the bonding mechanism as well as the internal microstructure of deposited splats and substrate as the function of temperature of spraying particles controlled by the nitrogen gas flow rate. The diverse microstructures of particles deposited at different nitrogen flow rates will be examined in the context of effects of the temperature of in-flight powder particles on the oxidation, grain size and structure, and bonding to the substrate.

2. Experimental

2.1 Feedstock Material, Spraying Process, and Conditions

Commercially available titanium powder (TILOP—45 μm, Sumitomo Titanium Corp., Tokyo, Japan) with near-spherical morphology was used. The powder has a Gaussian powder size distribution from 1 to 45 μm with the mean of 28 μm (volume average); the particle size was measured by the laser scattering method and confirmed by electron microscopy. Substrates were $5 \times 5 \times 5$ mm^3 cubes made of medium carbon steel (JIS: S45C, Fe-0.45 mass% C), which were grit-blasted with alumina powder and cleaned using acetone before making thick titanium coatings but were mirror polished for the preparation of splats. First of all, thick coatings in the thickness of about 400 μm were made via the warm spraying process by six passes of spray gun. Then, one layer of titanium particles was deposited on the mirror-polished surface of substrate via the spraying process by a single pass of spray gun in order to investigate the effects of particle temperature on the bonding of splats with the substrate and the microstructure within the splats. The spraying system used in this study is shown schematically in Fig. 1, which has been described in detail elsewhere (Ref 3, 9). The supersonic flow of combustion gas made from a mixture of kerosene and oxygen was mixed with nitrogen in order to lower the temperature of combustion gas in a chamber placed between the combustion chamber and the powder feeding ports. The process enables to heat the feedstock powder to higher temperatures as compared to the cold spray while avoiding melting the powder, which should be beneficial in terms of the deposition efficiency and the coating density for materials with the high melting point such as titanium (Ref 21). The nitrogen flow rate was varied in the range of 500-1500 dm^3/min. Spraying distance, defined as the distance from the end of spraying gun to the substrate in Fig. 1, was kept at 180 mm. The main spraying parameters used in this study are listed in Table 1.

Table 1 List of gas and fuel flow rates and spray parameters for the thick coating and the single splat of titanium

N_2, dm^3/min	Kerosine, dm^3/min	O_2, dm^3/min	Spray gun transverse velocity, mm/s (thick, single)	Powder feed rate, g/min (thick, single)
500	0.391	805	(700, 1500)	(27, 4)
1000	0.347	714	(700, 1500)	(27, 4)
1500	0.301	623	(700, 1500)	(27, 4)

2.2 Microstructure Observation

Microstructures of the thick titanium coating layer and the single titanium particles deposited on the substrate were, respectively, first observed by high resolution scanning electron microscopy (FE-SEM, JEOL JSM-6500). Prior to SEM observations, the titanium deposited sample was cut and prepared by standard metallographic techniques to reveal a transverse section. Back-scattered

electron (BSE) images were also obtained on the samples. In order to observe the high magnified image, TEM (JEOL JSM 2000FX) operating at 200 kV was used.

2.3 TEM Sample Preparation Using FIB Lift-Out Technique

The thin sample for TEM observations were made by the FIB lift-out technique in order to examine the microstructure and bonding of deposited titanium splat and substrate. With this FIB method, one can avoid the mechanical sawing and thinning. Furthermore, an electron-transparent membrane can be exquisitely milled at a desired location by the focused Ga^+ ions beam and finished in the same chamber without moving the sample. The typical procedure of sample preparation by the FIB lift-out technique is shown in Fig. 2. In order to make a TEM sample with the whole cross-sectional in one titanium splat, a small splat with about 5 μm diameter was selected in this case. A protective tungsten layer was deposited on the center of desired splat as shown in Fig. 2(a). After the tungsten deposition, graduated trenches were milled into the bulk specimen in the downward perpendicular direction of splat surface by the delicate controlled Ga^+ ions (Fig. 2b). The sides and the bottom of rough milled specimen were cut by the ions. A micromanipulator lifted out the cut sample and put on a copper grid (Fig. 2c). Finally, a thin electron-transparent sample was made after additional thin milling and cleaning (Fig. 2d).

3. Results and Discussion

3.1 Calculated Temperature and Velocity of Typical Titanium Particles and Obtained Cross Sections of Thick Titanium Coatings by Warm Spraying

The temperature and velocity of sprayed titanium particles of 30 μm diameter were calculated by the gas dynamics simulation at 500 and 1500 dm^3/min flow rates of nitrogen gas and shown in Fig. 3, respectively. The simulation method is described in detail elsewhere (Ref 22). The calculated temperatures of titanium particles at the substrate location of 180 mm are about 1250 and 850 °C, respectively, which imply that the nitrogen gas can lower effectively the temperature of in-flight titanium particles. On the other hand, the velocity of in-flight particles impacting onto a substrate was almost unchanged at the high velocity of about 750 m/s regardless of the nitrogen flow rate.

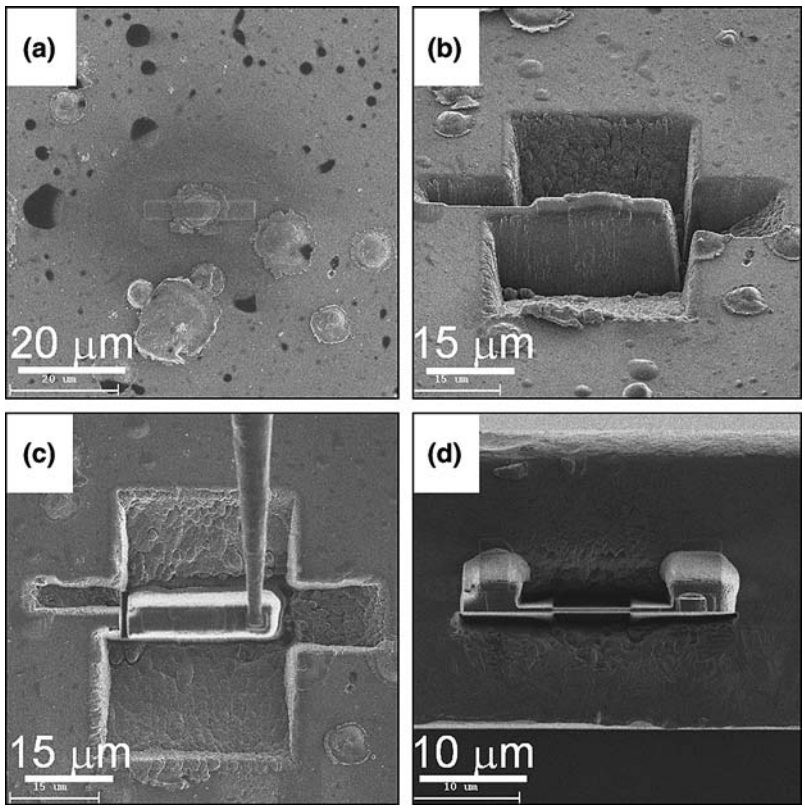

Fig. 2 Procedure of TEM sample preparation by the focused ion beam lift-out technique: (a) deposition of protective tungsten layer over the center of the interested splat, (b) graduated trenches milled into the bulk specimen, which will be cut on the sides and the bottom, (c) lifting-out of thickly milled sample and putting it on a copper grid by a micromanipulator, and (d) final thin sample after additional milling and cleaning

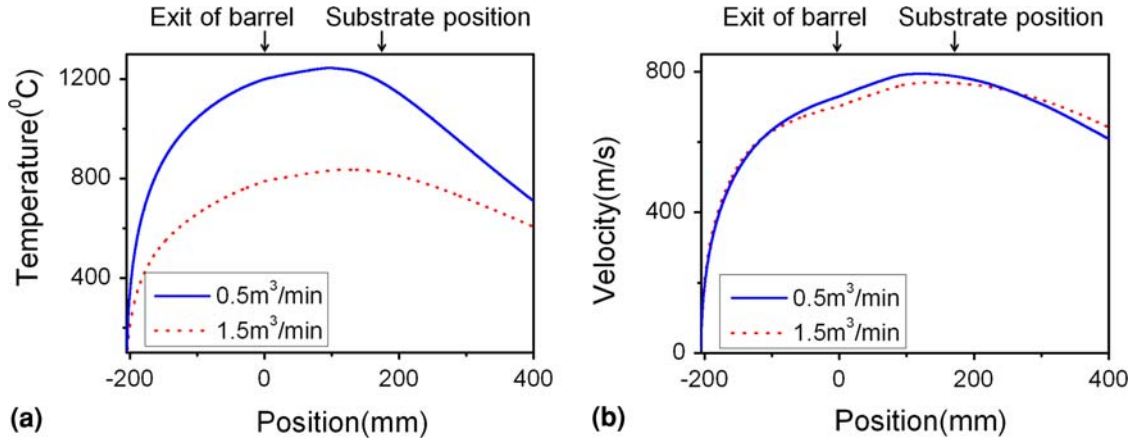

Fig. 3 Calculated in-flight temperature (a) and velocity (b) of 30 μm titanium particles sprayed at nitrogen flow rates of 500 and 1500 dm^3/min as functions of position. Position 0 corresponds to the exit of barrel of the warm spray apparatus. Spraying distance is defined as the distance between the end of barrel and the substrate, and was 180 mm in the study

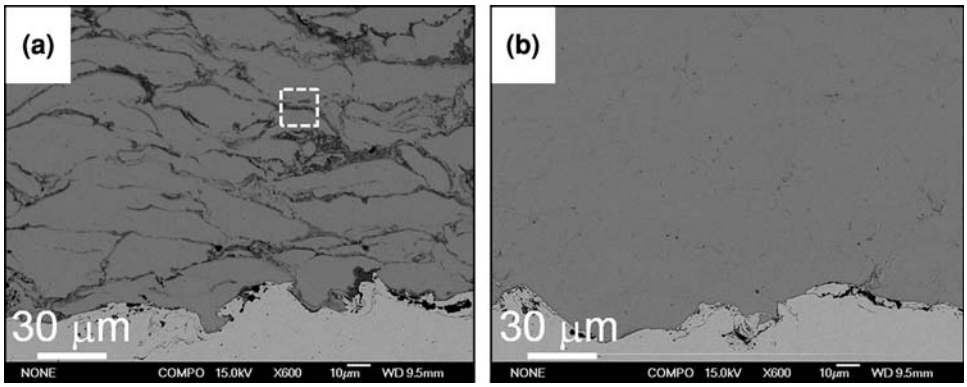

Fig. 4 Back-scattered electron images of cross section of the titanium coating layer and substrate deposited at different nitrogen flow rates: (a) 500 dm^3/min and (b) 1500 dm^3/min

Titanium coatings in the thickness of about 400 μm were prepared at various nitrogen flow rates for the cross-sectional observation as shown in Fig. 4. With the lowest flow rate of 500 dm^3/min, the boundaries of deformed particles can be observed with dark contrast in BSE images in Fig. 4(a). The gray boundaries surrounding each particle splat are oxide as shown in Fig. 5. The oxidation level at the low nitrogen flow rate is much higher than that of high flow rate. The result is in good agreement with the previous XRD result of the coating (Ref 3, 9). The oxide layers existing in the titanium coating can act as a barrier across the interface prohibiting the intimate bonding between the titanium and the substrate. As a result, the adhesive strength of the coating increased only slightly when the velocity of in-flight particle increased (Ref 10).

In comparison, there seems to be very little amount of oxides in the 1500 dm^3/min sample as shown in Fig. 4(b). In the figure, there was no recognizable gray boundary composed of oxide. The results indicate that the increase of nitrogen flow rate effectively suppressed the oxidation of titanium coating layers through the lower temperature of in-flight particles. In addition, the titanium coating layer obtained at 1500 dm^3/min was highly dense due to the low oxidation of in-flight titanium particles as well as the sufficient deformation at the impact achieved by the high velocity and the thermal softening of material (Ref 10, 21).

3.2 SEM Observation of Deposited Single Titanium Particles

Figure 6 shows SEM images of top-view of the deposited titanium particles, so-called as splat. At the lower nitrogen flow rate, diverse splat morphologies such as the unmelted (Fig. 6b), the disk-shaped (Fig. 6c), and the splashed splat (Fig. 6d) were observed side-by-side on a same mirror-polished substrate. The fraction of each splat type was measured by counting the number of each type of splats in the measured area of 1 × 1 mm^2. At the flow rate, the percentages of each splat type were, the unmelted: 44%, the disk-shaped: 29%, and the splashed: 27%, respectively.

Figure 7 shows the ratio of each splat shape at different nitrogen flow rates. As the nitrogen flow rate increased,

the percentages of disk-shaped and splashed splat decreased and most of the deposited splats became unmelted at 1500 dm^3/min. At the flow rate, particles at the much lower average temperature of about 850 °C appeared to be well deformed and adhered to the substrate regardless of the original powder size (Fig. 8). In addition, it is interesting that on the contrary to the result of low nitrogen flow rate, no disk-shaped or splashed splat were observed. This result indicates that at the low nitrogen flow rate some portion of the sprayed titanium particles reached the melting point and the diverse shapes of splats were formed on a substrate, whereas at the high nitrogen flow rate nearly all particles did not reach the melting point and were deposited in the solid state.

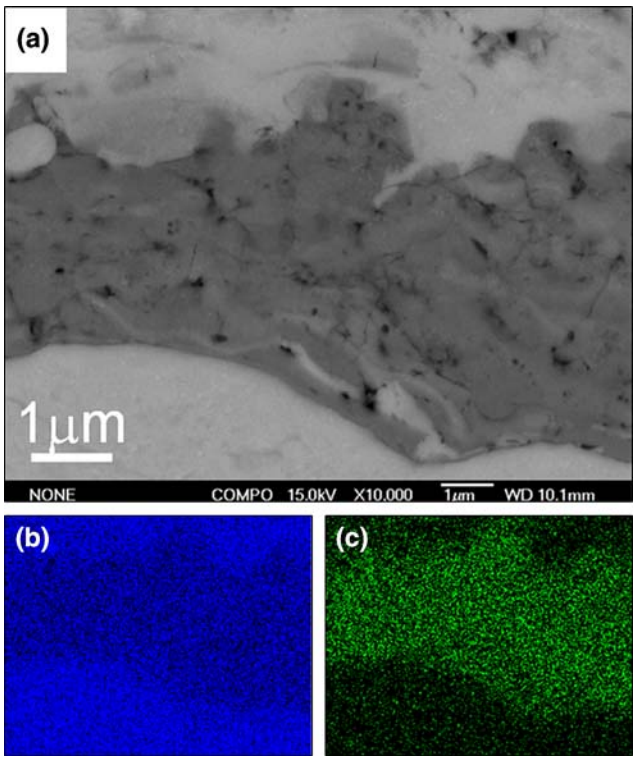

Fig. 5 Back-scattered electron image (a) and SEM/EDX elements mapping of titanium (b), and oxygen (c) at the marked region of Fig. 4(a)

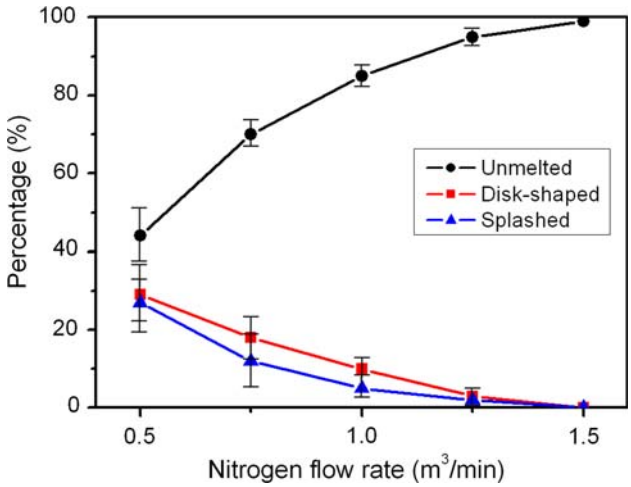

Fig. 7 Percentage of unmelted, disk-shaped, and splashed splats at various nitrogen flow rates

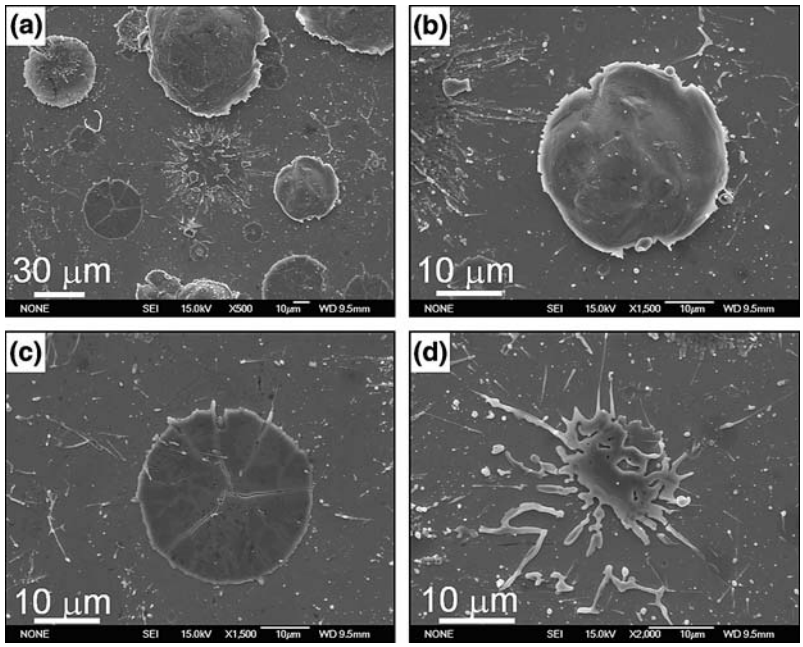

Fig. 6 Top-view of splats sprayed at a low nitrogen flow rate (500 dm^3/min): (a) general view at low magnification, (b) unmelted, (c) disk-shaped, and (d) splashed splat

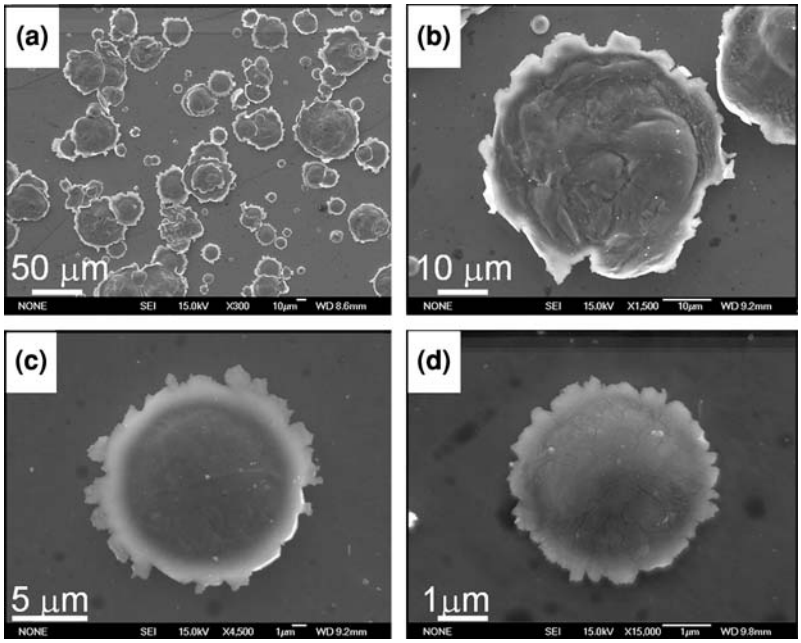

Fig. 8 Top-view (a) of splats sprayed at a high nitrogen flow rate (1500 dm^3/min), and magnified views of splats with different sizes of (b) ~50 μm, (c) ~15 μm, and (d) ~5 μm

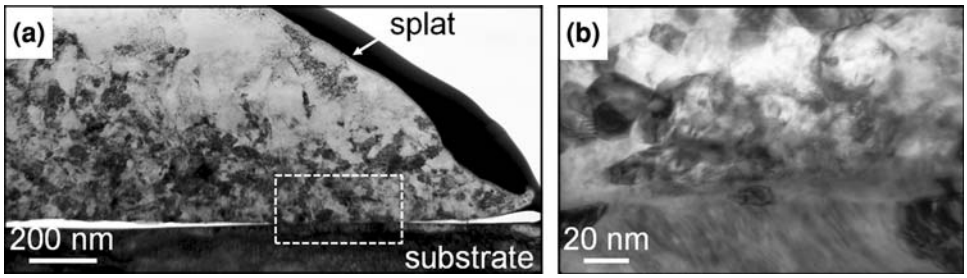

Fig. 9 Cross-sectional TEM image of unmelted sample (a) and close observation of bonded region marked with the dotted box in Fig. 9(a) (b). The black layer on the splat is a protective tungsten layer

3.3 TEM Observation of Single Titanium Particle

Figure 9 shows one half of the typical cross-sectional TEM sample of unmelted single splat. The splat could retain an as-sprayed shape after the TEM sample preparation without any Ga^+ ions induced damage. The microstructure shows that the titanium splat was heavily deformed as well as well-bonded to the substrate in the region marked by the dotted box. The high magnified image of bonded region clearly shows that the titanium splat and the substrate forms void-free interface (Fig. 9b). In addition, extremely fine grains were formed along the interfacial boundary of titanium/substrate in a single splat by dynamic recrystallization without any heat treatment (Ref 19). However, at the center-bottom region of single splat, a void was observed, which was believed to be formed by the elastic energy accumulated during impacting. The detailed void formation at the region will be published elsewhere.

The TEM sample of disk-shaped splat was also made by the same FIB method explained in Fig. 2. The sampling position was the center of single splat with about 20 μm diameter including a crack as shown in Fig. 6(c) (Fig. 10a). After the final milling and thinning, however, the region that electrons could be transparent was about 5 μm due to the limitation of sampling size to avoid bending the thin TEM sample. Figure 10(b) shows the cross-sectional microstructure of disk-shaped splat with the height of about 250 nm. Therefore, the aspect ratio defined as the height/diameter of disk-shaped splat (Ref 21) was 0.00125. Compared with the ratio of unmelted splat (about 0.2), the disk-shaped splat was very flattened by the impact of spraying titanium particle and substrate. It is interesting that at the interface of titanium/substrate, very small voids with the diameter of about 10 nm were regularly observed along the interfacial boundary (Fig. 10c). The voids could be formed by the evaporation of adsorbed water

molecules on the substrate, the entrapped air molecules during impacting, and/or the rapid postimpact depressurization, and the subsequent freezing (Ref 18, 23-25).

The TEM sample of splashed splat made by the same FIB technique shows a specific cross-sectional microstructure. The sampling position was the center of single splat with the diameter of about 5 μm including a small hole as shown in Fig. 11(a). The cross-sectional image shows that a large gap with the size of 50-100 nm existed between the titanium splat and the substrate (Fig. 11b) even though the splashed splat was partly adhered on the substrate. The gap was not made by the focused Ga^+ ion beam milling but by the impact and concomitant cooling process because the FIB milling was done in the downward direction to the surface of splat during the TEM sample preparation and the thickness of TEM sample at the bottom was thicker than that of upper region. Similar large gaps were also observed in the plasma-sprayed silicon (Ref 26) or yttria-stabilized zirconia (YSZ) splats made on cold substrates (Ref 18). It is believed that the poor wettability at the interface of splat and substrate resulted in the gap at the interface during cooling (Ref 23). However, further study on the interfacial microstructure would clarify the formation of gap between the sprayed particle and the substrate. As the height of splashed splat is 400 nm, the aspect ratio is about 0.02 (including the splashed arms) to 0.1 (the center region). It means that the splashed splat was slightly less flattened compared with the disk-shaped splat. Moreover, the heat conduction from the titanium splat into the substrate was slow due to the poor contact between the splat and the substrate. As a result, larger grains than that of disk-shaped splat were formed due to the slower cooling rate during the solidification as shown by the cross-sectional microstructure. It should be noted also that the substrate impacted by titanium particles was hardly deformed in the cases of the disk-shaped and the splashed splats.

The bonding formation between the spraying particle and the substrate is generally important because the intimate bonding of particle/substrate can result in not just the increased bonding strength, but also the dense coating layer. The unmelted and the disk-shaped splat were bonded with the substrate even though there are ultra fine voids formed along the interface of titanium/substrate of the disk-shaped splat. Especially, cracks were observed on the surface of disk-shaped splats (Fig. 6c) and on the through-thickness image (Fig. 10b). These cracks in the disk-shaped splats indicate that the adhesion between the titanium splat and the substrate was high because the cracking occurs to relieve the stress caused by the constraint of substrate on the splat shrinkage during quenching and cooling (Ref 25). In contrast, the splashed splat was not connected to the substrate.

A final point to note is that the ratio of disk-shaped splats to splashed splats remained almost 1 throughout this study. Fukumoto et al. has shown that the splat morphology of plasma-sprayed particles changes from the splashed to the disk-shaped as the substrate temperature is increased or as the ambient pressure is decreased. The substrate temperature and the ambient pressure at which the ratio of two splat types is equal to 1 are termed as the transition temperature and the transition pressure, respectively (Ref 27). The present result seems to imply that the temperature and the pressure for the molten titanium might be close to the room temperature and the atmospheric pressure, which is in agreement with Fukumoto's results, because no preheating of substrate and reduction of ambient pressure were provided in the present study. However, there are other factors to be considered in the warm spraying. The velocity of in-flight powder (about 750 m/s) is much higher than that of

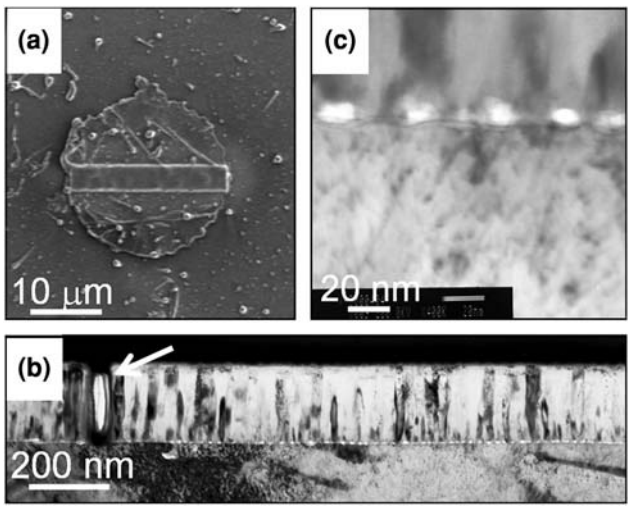

Fig. 10 Micrographs of disk-shaped splat: (a) deposition of protective tungsten layer over the center of desired splat, (b) cross-sectional TEM image near the interface of titanium/substrate, and (c) high magnified image of the interfacial region. The arrow indicate a crack formed in the disk-shaped splat

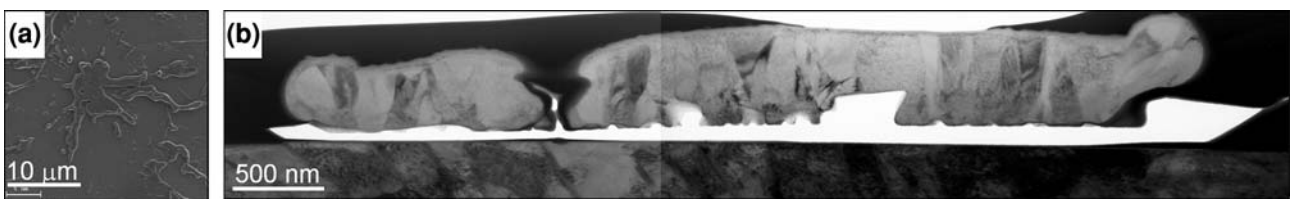

Fig. 11 Micrographs of splashed splat: (a) top-view of desired splat for the TEM sampling and (b) cross-sectional TEM image of a whole splat

atmospheric plasma-sprayed powder (about 100 m/s) (Ref 27), as well as the dynamic gas pressure on the substrate is very high due to the high velocity of propellant jet (Ref 28). These high particle velocity and gas pressure might affect the transition phenomena and further study is needed to clarify the point.

4. Conclusions

Effects of temperature of in-flight particles on the bonding and the microstructure of warm-sprayed titanium coatings and splats were investigated. In the process, nitrogen gas was mixed with the HVOF flame jet to control the temperature of propellant gas. It was found that at the lower nitrogen flow rate of 500 dm^3/min, some portion of the sprayed titanium particles reached the melting point and three types of splats, i.e., the unmelted, the disk-shaped, and the splashed, were formed on a substrate. As the nitrogen flow rate increased, the ratio of disk-shaped and splashed splats decreased; especially, at 1500 dm^3/min, most of the deposited splats became unmelted, which were well deformed and adhered to the substrate regardless of the original powder size. The results clearly indicate that the temperature of sprayed powder at the moment of impact onto the substrate was significantly changed in the warm sparying as predicted by the gas dynamic simulation.

The TEM observation of splats revealed distinctively different microstructures depending on the type of splats. In the unmelted splat, extremely fine grains were formed along the interfacial boundary between the titanium and the steel substrate by dynamic recrystallization and a void was observed at the center-bottom region of splat. The disk-shaped splat showed a columnar structure and very small voids with the diameter of about 10 nm were densely distributed along the interfacial boundary of splat/substrate. The splashed splat showed larger grains than that of disk-shaped splat due to the poor contact between the splat and the substrate exemplified by the large gap of 50-100 nm size and the slow cooling rate resulted from the limited hear conduction to the substrate during the solidification. The substrate impacted by titanium particles was hardly deformed in the cases of the disk-shaped and the splashed splats indicating that these particles were molten at the moment of impact.

These results clearly demonstrated the efficacy of warm spraying for controlling the microstructure of titanium coatings by varying the temperature of sprayed particles at the impact, which was made possible by the relatively simple modification of commercially available HVOF apparatus. In terms of forming a densely packed and adherent coating, tuning the particle temperature slightly below the melting point so that most of the particles were softened but not melted should be effective because of the controlled oxidation and consistent internal as well as interfacial structure. Such merit of warm spraying demonstrated for titanium in this study is expected to be applicable to wider range of materials whose deformability increases in the temperature range 500-2000 °C.

Acknowledgments

The authors would like to acknowledge Prof. Sanjay Sampath of SUNY Stony Brook University for his advice on the microstructural characteristic of deposited splats, and Ms Kawano and Mr Komatsu of NIMS for sample preparations. This research was supported by the Nanotechnology Network Program of Ministry of Education, Culture, Sports, Science and Technology of the Japanese Government and KAKENHI 19360335.

References

1. M. Grujicic, J. R. Saylor, D. E. Beasley, W. S. DeRosset, and D. Helfritch, Computational Analysis of the Interfacial Bonding between Feed-Powder Particles and the Substrate in the Cold-Gas Dynamic-Spray Process, *Appl. Surf. Sci.*, 2003, **219**(3-4), p 211-227
2. C. Borchers, F. Gärtner, T. Stoltenhoff, H. Assadi, and H. Kreye, Microstructural and Macroscopic Properties of Cold Sprayed Copper Coatings, *J. Appl. Phys.*, 2003, **93**(12), p 10064-10070
3. J. Kawakita, S. Kuroda, T. Fukushima, H. Katanoda, K. Matsuo, and H. Fukanuma, Dense Titanium Coatings by Modified HVOF Spraying, *Surf. Coat. Tech.*, 2006, **201**(3-4), p 1250-1255
4. A. Papyrin, V. Kosarev, S. Klinkov, A. Alkhimov, and V. Fomin, *Cold Spray Technology*, Elsevier, Amsterdam, 2007
5. T. Schmidt, F. Gärtner, H. Assadi, and H. Kreye, Development of a Generalized Parameter Window for Cold Spray Deposition, *Acta Mater.*, 2006, **54**(3), p 729-742
6. T. Marrocco, D.G. McCartney, P.H. Shipway, and A.J. Sturgeon, Production of Titanium Deposits by Cold-Gas Dynamic Spray: Numerical Modeling and Experimental Characterization, *J. Therm. Spray Technol.*, 2006, **15**(2), p 263-272
7. P. Fauchais and G. Montavon, Plasma Spraying: From Plasma Generation to Coating Structure, *Adv. Heat. Transfer.*, 2007, **40**, p 205-344
8. A.A. Syed, A. Denoirjean, P. Fauchais, and J.C. Labbe, On the Oxidation of Stainless Steel Particles in the Plasma Jet, *Surf. Coat. Tech.*, 2006, **200**(14-15), p 4368-4382
9. S. Kuroda, J. Kawakita, M. Watanabe, and H. Katanoda, Warm Spraying—A Novel Coating Process based on the High-Velocity Impact of Solid Particles, *Sci. Technol. Adv. Mat.*, 2008, **9**(3), p 033002 (17 p)
10. K.H. Kim, M. Watanabe, K. Mitsuishi, J. Kawakita, T. Wu, and S. Kuroda, Microstructure Observation on the Interface between Warm Spray Deposited Titanium Powder and Steel Substrate, *International Thermal Spray Conference and Exposition 2008: Thermal Spray Crossing Borders*, E. Lugscheider, Ed., June 2-4, ASM International, Maastricht, The Netherlands, 2008, CD-ROM, p 1289-1294
11. A. Sharma, R.J. Gambino, and S. Sampath, Anisotropic Electrical Properties in Thermal Spray Metallic Coatings, *Acta Mater.*, 2006, **54**(1), p 59-65
12. K. Balani, A. Agarwal, S. Seal, and J. Karthikeyan, Transmission Electron Microscopy of Cold Sprayed 1100 Aluminum Coating, *Scripta Mater.*, 2005, **53**(7), p 845-850
13. M. Grujicic, C.L. Zhao, W.S. DeRosset, and D. Helfritch, Adiabatic Shear Instability based Mechanism for Particles/Substrate Bonding in the Cold-Gas Dynamic-Spray Process, *Mater. Des.*, 2004, **25**(8), p 681-688
14. C.J. Li, W.Y. Li, and Y.Y. Wang, Formation of Metastable Phases in Cold-Sprayed Soft Metallic Deposit, *Sur. Coat. Tech.*, 2005, **198**(1-3), p 469-473
15. C. Borchers, F. Gärtner, T. Stoltenhoff, and H. Kreye, Microstructural Bonding Features of Cold Sprayed Face Centered Cubic Metals, *J. Appl. Phys.*, 2003, **93**(8), p 4288-4292
16. Y. Xiong, K. Kang, G. Bae, S. Yoon, and C. Lee, Dynamic Amorphization and Recrystallization of Metals in Kinetic Spray Process, *Appl. Phys. Lett.*, 2008, **92**(19), p 194101 (3 p)

17. A.C. Hall, L.N. Brewer, and T.J. Roemer, Preparation of Aluminum Coatings Containing Homogeneous Nanocrystalline Microstructures Using the Cold Spray Process, *J. Therm. Spray Technol.*, 2008, **17**(3), p 352-359
18. T. Chraska and A. H. King, Effect of Different Substrate Conditions upon Interface with Plasma Sprayed Zirconia—A TEM Study, *Surf. Coat. Tech.*, 2002, **157**(2-3), p 238-246
19. K.H. Kim, M. Watanabe, J. Kawakita, and S. Kuroda, Grain Refinement in a Single Titanium Powder Particle Impacted at High Velocity, *Scripta Mater.*, 2008, **59**(7), p 768-771
20. L.A. Giannuzzi and F.A. Stevie, A Review of Focused Ion Beam Milling Techniques for TEM Specimen Preparation, *Micron*, 1999, **30**(3), p 197-204
21. K.H. Kim, M. Watanabe, and S. Kuroda, Thermal Softening Effect on the Deposition Efficiency and Microstructure of Warm Sprayed Metallic Powder, *Scripta Mater.*, 2009, doi:10.1016/j.scriptamat.2008.12.050
22. J. Kawakita, H. Katanoda, M. Watanabe, K. Yokoyama, and S. Kuroda, Warm Spraying: An Improved Spray Process to Deposit Novel Coatings, *Surf. Coat. Tech.*, 2008, **202**(18), p 4369-4373
23. M. Qu, Y. Wu, V. Srinivasan, and A. Gouldstone, Observations of Nanoporous Foam Arising from Impact and Rapid Solidification of Molten Ni Droplets, *Appl. Phys. Lett.*, 2007, **90**(25), p 254101 (3 p)
24. C.-J. Li and J.-L. Li, Evaporated-Gas-Induced Splashing Model for Splat Formation During Plasma Spraying, *Surf. Coat. Tech.*, 2004, **184**(1), p 13-23
25. X. Jiang, Y. Wan, H. Herman, and S. Sampath, Role of Condensates and Adsorbates on Substrate Surface on Fragmentation of Impinging Molten Droplets During Thermal Spray, *Thin Solid Films*, 2001, **385**(1-2), p 132-141
26. B.D. Kharas, G. Wei, S. Sampath, and H. Zhang, Morphology and Microstructure of Thermal Plasma Sprayed Silicon Splats and Coatings, *Surf. Coat. Tech.*, 2006, **201**(3-4), p 1454-1463
27. M. Fukumoto, T. Yamaguchi, M. Yamada, and T. Yasui, Splash Splat to Disk Splat Transition Behavior in Plasma-Sprayed Metallic Materials, *J. Therm. Spray Technol.*, 2007, **16**(5-6), p 905-912
28. V.R. Srivatsan and A. Dolatabadi, Simulation of Particle-Shock Interaction in a High Velocity Oxygen Fuel Process, *J. Therm. Spray Technol.*, 2006, **15**(4), p 481-487